

One-pot hydrothermal synthesis of nitrogen-doped hierarchically porous carbon monoliths for supercapacitors

Yurong Liu

Published online: 19 September 2014
© Springer Science+Business Media New York 2014

Abstract The nitrogen-doped hierarchically porous carbon monoliths (N-HPCMs) were successfully synthesized by using dicyandiamide (DCDA) as nitrogen source, phenolic resol as carbon precursor and mixed triblock copolymers as templates via a one-pot hydrothermal approach. The obtained carbon monoliths possess tunable mesopore size (4.3–11.4 nm), large surface area (552–660 m²/g), and high nitrogen content (up to 12.1 wt%). Ascribed to the nitrogen-doped frameworks and hierarchical porosity, N-HPCMs exhibit good electrochemical performance as the supercapacitor electrode with specific capacitance of 268.9 F/g (in 6 M KOH) at a current density of 1 A/g, and a 4.1 % loss of the specific capacitance after 5,000 charge–discharge cycles, indicating a long-term cycling stability. Such unique features make N-HPCMs promising electrode materials for high performance supercapacitors.

Keywords Nitrogen-doped carbon monoliths · Hydrothermal synthesis · Hierarchically porous · Supercapacitors

1 Introduction

As a new kind of energy-storage devices, supercapacitors have recently attracted increasing attention due to their high power density and long cycle life [1]. Because of high porosity and large surface area, porous carbon materials

have been regarded as one of the most promising candidates for supercapacitor electrodes. To date, activated carbons are the most commonly used electrode materials for supercapacitors [2]. However, they suffer from a drawback of slow mass transfer due to the small micropores (<2 nm) and long diffusion pathways [3]. While, the mesopores (2–50 nm) can afford a short ion-transport pathway with a minimized resistance, and the macropores (>50 nm) are beneficial for the formation of ion-buffering reservoirs giving a decreased diffusion distance [4–11]. The combination of multi-level pores (micro-, meso-, and macropores) in carbon materials is expected to provide a harmonious electrochemical environment for the full realization of fast ion transport and high charge storage capability. Therefore, great endeavors have been made to design hierarchically porous carbons containing two or three types of pores and characterize their electrochemical capacitive properties [12–19].

However, most of the hierarchically porous carbon monoliths have hydrophobic surface and a limited number of specific active sites, which impedes their practical application. It has been demonstrated that the incorporation of nitrogen atoms into the carbon matrix not only changes the electronic properties of carbons but also produces additional functional groups on the carbon surface to improve the wettability, which consequently enhance the electrochemical performance of carbon materials [20–24]. Until now, some works have been reported on electrochemical properties of nitrogen-doped hierarchically porous carbon powders prepared mainly through nanocasting method [25] or chemical activation route [26]. The electrodes of these carbon materials are usually fabricated using a mixture of carbon powders and binders which lower the electrical conductivity and the electrodes are possibly broken into fragments during the charge–

Y. Liu (✉)
Chongqing Key Laboratory of Micro/Nano Materials Engineering and Technology, Research Center for Material Interdisciplinary Science, Chongqing University of Arts and Science, Chongqing 402160, People's Republic of China
e-mail: liuyr1978@163.com

discharge cycles. In contrast to carbon powders, carbon monoliths are more advantageous for supercapacitors because no binders are needed due to their continuous skeletons [27].

To the best of our knowledge, there are still few works about the synthesis of nitrogen-doped hierarchically porous carbon monoliths (N-HPCMs) and the evaluation of their electrochemical properties [28]. To find a facile one-pot method to fabricate N-HPCMs is still challenging. In this report, we demonstrate a one-pot hydrothermal synthesis of N-HPCM by using dicyandiamide (DCDA) as nitrogen source, phenolic resol as carbon precursor and mixed triblock copolymers as templates. Furthermore, the electrochemical performance of N-HPCM-based electrodes has been systematically investigated. This facile and economical hydrothermal synthesis approach can be useful for the large-scale industrial production of porous carbon monolith materials with nitrogen-doped frameworks and hierarchical porosity for supercapacitor applications.

2 Experimental

2.1 Materials

Triblock copolymers Pluronic P123 ($M_w = 5,800$, EO₂₀-PO₇₀-EO₂₀) and Pluronic F127 ($M_w = 12,600$, EO₁₀₆-PO₇₀-EO₁₀₆) were purchased from Acros Corp. DCDA, phenol, formalin (37 wt%) and ethanol were purchased from Chongqing Huanwei Chemical Corp. All chemicals were used as received without purification.

2.2 Synthesis of N-HPCMs

The synthesis of N-HPCMs was carried out under hydrothermal conditions by using phenolic resols as carbon precursors, DCDA as nitrogen source and the mixed triblock copolymers as templates. Typically, 1.0 g of phenol and 3.5 mL of a formaldehyde solution (37 wt%) were dissolved in 5 mL of 0.5 M NaOH solution and stirred at 70 °C for 0.5 h. Then, an aqueous solution of mixed triblock copolymers (0.75 g P123 and 1.25 g F127 in 10 mL of water) and different amounts of DCDA (0–0.7 g) were added to the above solution, and the mixture was continuously stirred at 70 °C for 3 h. After that, the solution was poured into an autoclave and transferred into an oven at 100 °C for 12 h. The obtained polymeric monolith was collected by filtration, washed with water and dried in vacuum. The pyrolysis was carried out in a tubular furnace under N₂ atmosphere at 600 °C for 3 h with a ramp rate of 1 °C/min. The samples were denoted as N-HPCM-x, where x was the mass of DCDA (g).

2.3 Characterization

Scanning electron microscopy (SEM) images were collected with a Hitachi S-3400N electron microscope operated at 20 kV. Transmission electron microscopy (TEM) experiments were conducted on a JEOL 2011 microscope operated at 200 kV. N₂ adsorption–desorption was determined using a Tristar-3020 surface area analyzer. Nitrogen content analysis was carried out on an elemental analyzer (Vario EL III, Elementar).

2.4 Electrochemical measurements

The electrochemical experiments were carried out using a three-electrode system, employing platinum as the counter electrode, the saturated calomel electrode (SCE) as reference electrode and 6 M KOH solution as the electrolyte. The working electrode was prepared by fixing a thin piece of as-prepared carbon samples on a platinum plate. The cyclic voltammetry (CV), galvanostatic charge–discharge (GCD) and electrochemical impedance spectroscopy (EIS) tests were performed on a CHI 660D electrochemical analyzer at ambient conditions.

3 Results and discussion

3.1 Morphology and porous structure

Photographs of the as-synthesized polymeric monolith and the corresponding calcined carbon monolith (N-HPCM-0.3) show a very stable and crack-free bulk macroscopic appearance (Fig. 1). The polymeric monolith in Fig. 1a is 2.8 cm in diameter and 1.6 cm in height. After high-temperature calcination and removal of templates, the nitrogen-doped carbon monolith N-HPCM-0.3 maintains the regular cylinder-like shape (2.4 cm in diameter and 1.2 cm in height). The volume shrinkage is calculated to be about 45 %. The N-HPCM samples also have some degree of mechanical strength and can be cut into small pieces. So, it is convenient to test their supercapacitive properties without any conductive additive and binder.

SEM images (Fig. 2a, b) show that the structures of the as-synthesized polymeric monoliths are constructed from interconnected particles. These particles build up a 3-D macroporous framework, with sizes in the range of 2–6 μm. After carbonization at 600 °C under N₂ atmosphere for 3 h, the macropore size of carbon monolith slightly increases (Fig. 2c, d). TEM images of N-HPCM-0.3 sample (Fig. 3) reveal that these building blocks are of an ordered 2-D hexagonal mesostructure.

Fig. 1 Photographs of (a) the as-synthesized polymeric monolith and (b) the corresponding calcined carbon monolith (N-HPCM-0.3)

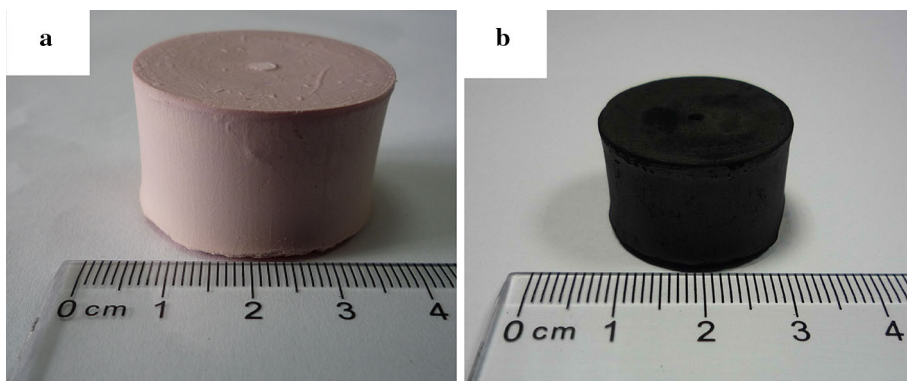


Fig. 2 SEM images of (a, b) the as-synthesized polymeric monolith and (c, d) the corresponding calcined carbon monolith (N-HPCM-0.3)

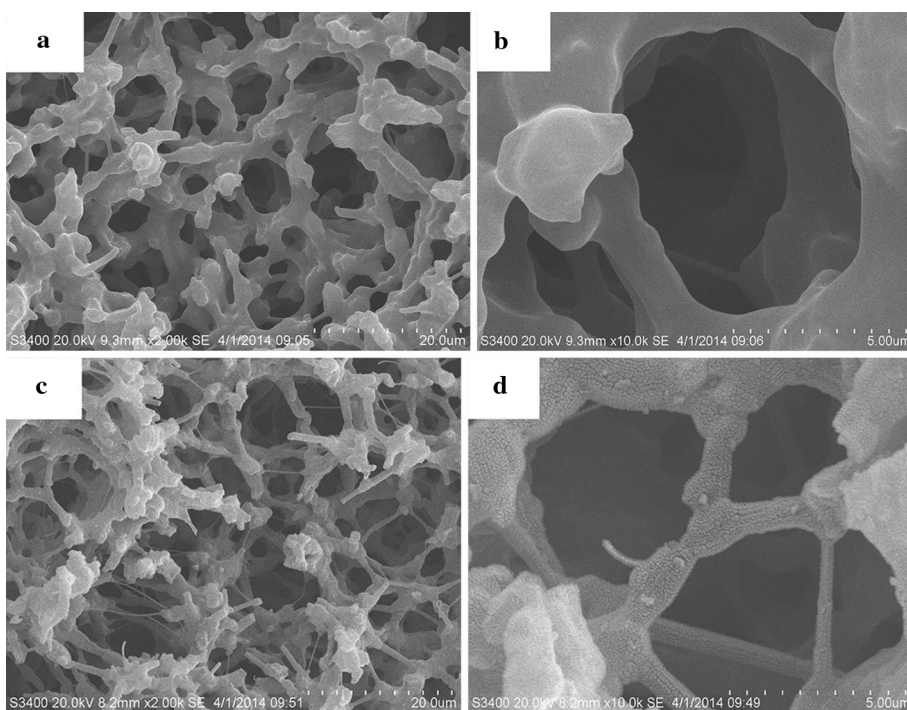
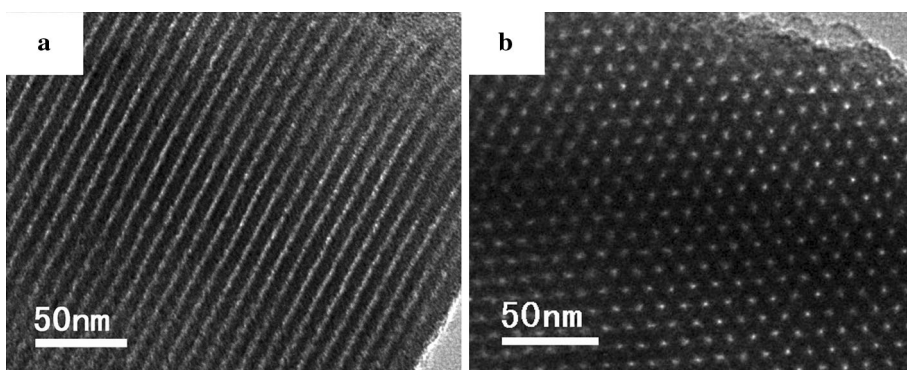


Fig. 3 TEM images of N-HPCM-0.3 sample viewed from (a) [10] and (b) [11] directions



N_2 adsorption–desorption isotherms and pore size distribution of the carbon monoliths after calcination at 600 °C are shown in Fig. 4. N_2 adsorption–desorption

isotherms of the sample H-NMC-0 without adding DCDA show type-IV curves with a sharp capillary condensation step in the relative pressure range of 0.4–0.6 and H_1 -type

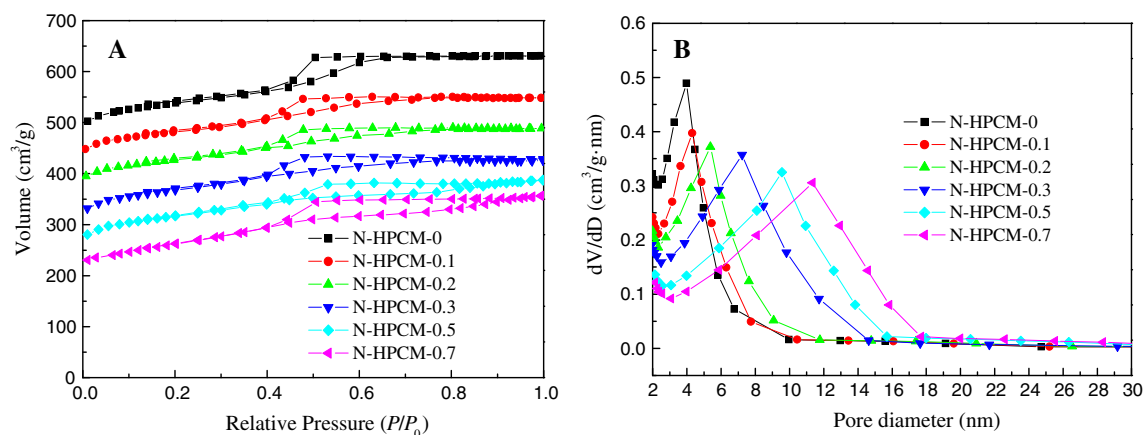


Fig. 4 N_2 adsorption–desorption isotherms (a) and pore size distribution (b) of N-HPCM samples. For clarity, the isotherms curves in (A) are offset by $350 \text{ cm}^3/\text{g}$ for N-HPCM-0, $300 \text{ cm}^3/\text{g}$ for N-HPCM-

0.1, $250 \text{ cm}^3/\text{g}$ for N-HPCM-0.2, $200 \text{ cm}^3/\text{g}$ for N-HPCM-0.3, $150 \text{ cm}^3/\text{g}$ for N-HPCM-0.5, $100 \text{ cm}^3/\text{g}$ for N-HPCM-0.7

Table 1 Textural properties of N-HPCM samples

Sample	$S_{\text{BET}}^{\text{a}}$ (m^2/g)	V_t^{b} (cm^3/g)	$V_{\text{micro}}^{\text{c}}$ (cm^3/g)	D^{d} (nm)	N content (wt%)
N-HPCM-0	688	0.45	0.23	3.8	0
N-HPCM-0.1	660	0.46	0.24	4.3	1.9
N-HPCM-0.2	632	0.49	0.24	5.4	4.5
N-HPCM-0.3	597	0.53	0.25	7.2	6.9
N-HPCM-0.5	573	0.61	0.25	9.6	9.7
N-HPCM-0.7	552	0.66	0.25	11.4	12.1

^a BET specific surface area

^b Total pore volume

^c Microporous pore volume

^d BJH desorption average pore diameter

hysteresis loop, indicative of uniform cylindrical pores. After the addition of DCDA, the capillary condensation step shifts to high relative pressure ranges, indicating that the pore size increases gradually. As the mass of DCDA increases from 0.1 to 0.7 g, the pore size dramatically increases from 4.3 to 11.4 nm (Fig. 4b; Table 1), indicating that higher amounts of DCDA can dramatically cause the expansion of mesopores. According to the literature [29], the larger pore size is beneficial to the accesses of electrolyte into the pores and ionic transportation. The BET surface area and pore volume of nitrogen-doped carbon monoliths are in the ranges of $552\text{--}660 \text{ m}^2/\text{g}$ and $0.46\text{--}0.66 \text{ cm}^3/\text{g}$, respectively (Table 1). However, when the mass of DCDA is further increased ($>0.7 \text{ g}$), the ordered mesostructures of N-HPCMs are degenerated.

3.2 Electrochemical performance

Figure 5 shows CV curves of N-HPCM-based electrodes at a sweep rate of 5 mV/s in 6 M KOH aqueous solution. For

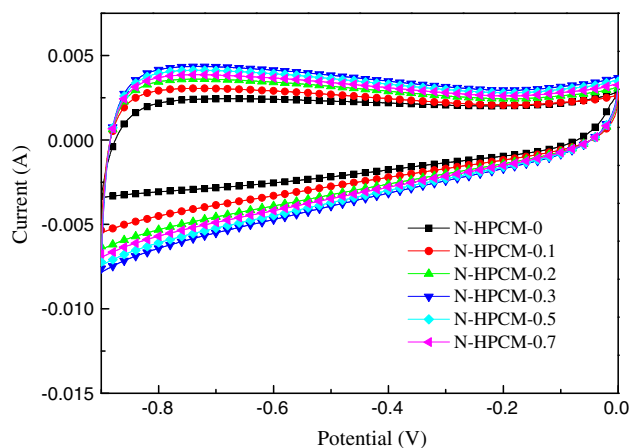


Fig. 5 CV curves of the carbon monoliths in 6 M KOH at the scan rate of 5 mV/s

comparison, the CV curve of N-HPCM-0 is also included. It can be observed that all curves present a quasi-rectangular voltammogram shape, which indicates that N-HPCM materials have good electrochemical capacitive properties. It is noteworthy that the excellent supercapacitive performance can be ascribed to their hierarchical pore structure which facilitates fast mass transportation and decreases ion-transport resistance. Besides, the nitrogen-doped carbon monolithic electrodes possess the bigger inner integrated area than nitrogen-undoped electrode (N-HPCM-0). In general, at the same scan rate, a larger inner integrated area of the CV curve indicates a higher specific capacitance.

Figure 6 exhibits the GCD curves of the carbon monoliths at the current density of 1 A/g in 6 M KOH aqueous solution. It can be clearly seen that these charge–discharge curves are closely linear and show a typical triangle symmetrical distribution, revealing a good supercapacitive behavior and electrochemical reversibility, which is in well agreement

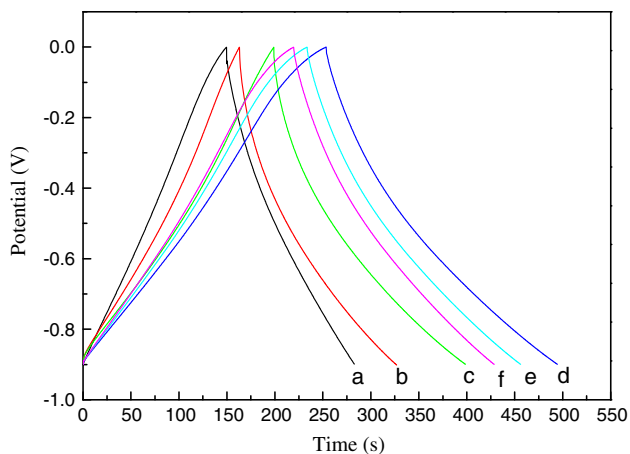


Fig. 6 GCD curves of the carbon monoliths at the current density of 1 A/g (a N-HPCM-0, b N-HPCM-0.1, c N-HPCM-0.2, d N-HPCM-0.3, e N-HPCM-0.5, f N-HPCM-0.7)

with CV observations. Nevertheless, the charge–discharge time in one cycle of N-HPCM-0.3 electrode is much longer than that of N-HPCM-0 electrode, which directly indicates an obvious improvement in capacitance properties after the incorporation of nitrogen atoms.

The specific capacitance values for N-HPCM-0 and N-HPCM-0.3 electrodes obtained from the charge–discharge curves are shown in Fig. 7. The specific capacitance of N-HPCM-0.3 (268.9 F/g) at low current density of 1 A/g is higher than that of N-HPCM-0 sample without nitrogen modification (147.9 F/g), which suggests that the supercapacitive performance is greatly improved due to the incorporation of nitrogen into the carbon framework. The doped nitrogen can improve the wettability and modify the electronic properties of the carbon monoliths, thus leading to excellent supercapacitive performances. It should be noted that the specific capacitance of N-HPCM-0.3 electrode can still remain 229.4 F/g at a high loading current density of 5 A/g with the retention of 85 %, which indicates that the typical N-HPCM-0.3 sample as electrode material has a good rate capability.

An important criterion for supercapacitor electrode is its cycling life. The cycling life tests over 5,000 cycles for the N-HPCM-0 and N-HPCM-0.3 electrode at a current density of 1 A/g are carried out using GCD techniques (Fig. 8). The N-HPCM-0.3 electrode shows 4.1 % loss in the specific capacitance after 5,000 charge–discharge cycles. The decay of specific capacitances probably results from the irreversible reactions of electrolyte with the functional groups and the adsorbed impurities on the surface of the carbon monolith materials [31, 32]. Nevertheless, the N-HPCM-0.3 sample has good cycle performances due to the hierarchically porous structure providing low-resistant pathways and short distance for ions through the porous particles.

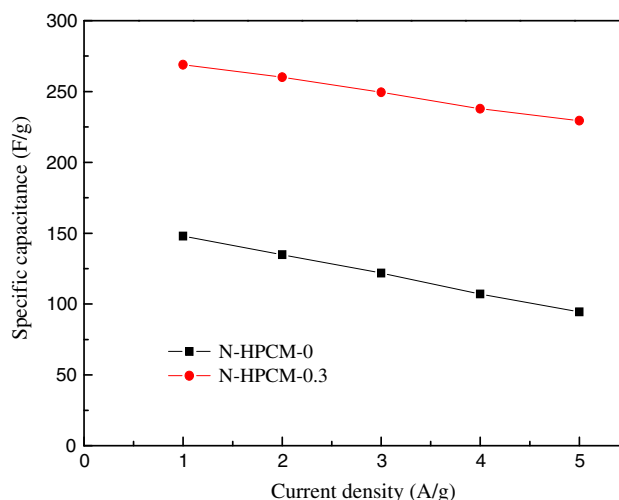


Fig. 7 Dependence of specific capacitance and current density for N-HPCM electrodes

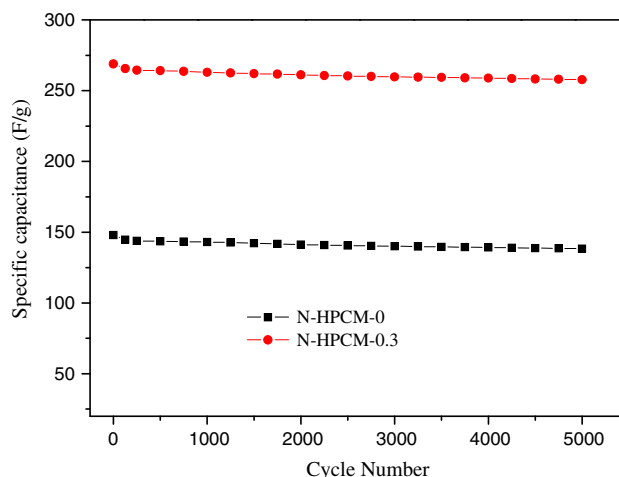


Fig. 8 Cycle life of the N-HPCM electrodes at a current density of 1 A/g

In order to evaluate the resistance which is related to the conductive properties, the N-HPCM electrodes are investigated by EIS measurement. As shown in Fig. 9, the impedance plots exhibit two distinct parts including a semicircle in high-frequency region and a sloped line in low-frequency region. The resistance of a supercapacitor, namely equivalent series resistance (ESR), consists of electronic contributions and ionic contributions [30]. The electrolyte resistance (R_s) calculated from the crossover point of the high frequency with the real part of the impedance is 0.52 and 0.26 Ω for N-HPCM-0 and N-HPCM-0.3 electrodes, respectively. Ionic or charge transfer resistances (R_{ct}) estimated from the diameter of semicircle is 0.17 and 0.12 Ω for N-HPCM-0 and

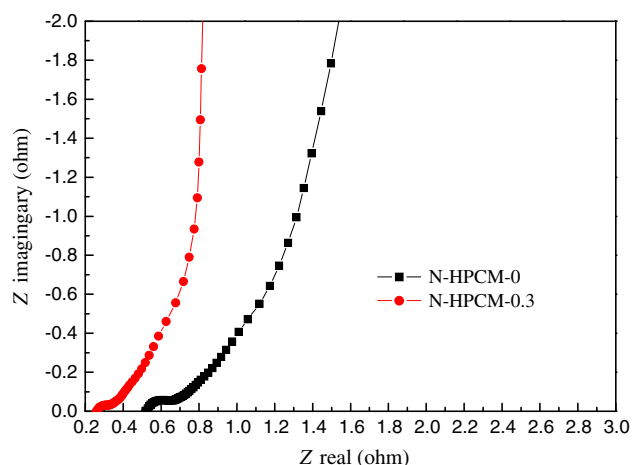


Fig. 9 Nyquist plots of N-HPCM electrodes with the frequency range from 100 kHz to 10 mHz

N-HPCM-0.3, respectively. These results suggest that the nitrogen-doped carbon monoliths have better conductive properties and consequent excellent electrochemical performance, which matches to the results of the CV and GCD measurements.

4 Conclusions

In summary, we demonstrate a one-pot hydrothermal method to synthesize nitrogen-doped carbon monoliths with hierarchically porous structures by using phenolic resol as carbon precursor, DCDA as nitrogen source, and mixed triblock copolymers as templates. The obtained carbon monoliths show an ordered 2-D hexagonal mesostructure with large pore size, 3-D macroporous scaffolds, and high nitrogen content. The hierarchically porous structure and doped nitrogen endow the carbon monoliths with high specific capacitance, excellent rate capability and cycle durability. This one-pot hydrothermal approach is of considerable importance for the large-scale production of nitrogen-doped hierarchical porous carbon monolithic materials for high performance supercapacitors.

Acknowledgments The authors gratefully acknowledge the financial supports from the Program of Chongqing Municipal Education Commission (KJ121201), the First Excellent Young Teachers Program of Chongqing high school ([2011]65), Chongqing Yongchuan Key Technologies R&D Program (YCSTC, 2011AC4001) and Research Program of Chongqing University of Arts and Sciences (Z2011RCYJ04).

References

1. W.C. Li, G.Z. Nong, A.H. Lu, H.Q. Hu, *J. Porous Mater.* **18**, 23 (2011)
2. D. Qu, *J. Power Sources* **109**, 403 (2002)
3. A.G. Pandolfo, A.F. Hollenkamp, *J. Power Sources* **157**, 11 (2006)
4. H. Zhou, S. Zhu, M. Hibino, I. Honma, *J. Power Sources* **122**, 219 (2003)
5. S. Alvarez, J. Esquena, C. Solans, A.B. Fuertes, *Adv. Eng. Mater.* **6**, 897 (2004)
6. A.H. Lu, J.H. Smatt, S. Backlund, M. Linden, *Microporous Mesoporous Mater.* **72**, 59 (2004)
7. L.F. Wang, S. Lin, K.F. Lin, C.Y. Yin, D.S. Liang, Y. Di, P.W. Fan, D.Z. Jiang, F.S. Xiao, *Microporous Mesoporous Mater.* **85**, 136 (2005)
8. A.H. Lu, W.C. Li, W. Schmidt, F. Schuth, *Microporous Mesoporous Mater.* **95**, 187 (2006)
9. M. Jaroniec, J. Choma, J. Gorka, A. Zawislak, *Chem. Mater.* **20**, 1069 (2007)
10. C. Ho, M. Wu, *J. Phys. Chem. C* **115**, 22068 (2011)
11. G.J. Tao, L.X. Zhang, Z.L. Hua, Y. Chen, L.M. Guo, J.M. Zhang, Z. Shu, J.H. Gao, H.R. Chen, W. Wu, Z.W. Liu, J.L. Shi, *Carbon* **66**, 547 (2014)
12. Y. Huang, H.Q. Cai, D. Feng, D. Gu, Y.H. Deng, B. Tu, H.T. Wang, P.A. Webley, D.Y. Zhao, *Chem. Commun.* **23**, 2641 (2008)
13. D. Carriazo, F. Picó, M.C. Gutiérrez, F. Rubio, J.M. Rojo, F. del Monte, *J. Mater. Chem.* **20**, 773 (2010)
14. H. Xu, Q.M. Gao, H.L. Guo, H.L. Wang, *Microporous Mesoporous Mater.* **133**, 106 (2010)
15. J. Balach, M.M. Bruno, N.G. Cotella, D.F. Acevedo, C.A. Barbero, *J. Power Sources* **199**, 386 (2012)
16. B.Z. Fang, A. Bonakdarpour, M.S. Kim, J.H. Kim, D.P. Wilkinson, J.S. Yu, *Microporous Mesoporous Mater.* **182**, 1 (2013)
17. Y. Li, Z.Y. Fu, B.L. Su, *Adv. Funct. Mater.* **22**, 4634 (2012)
18. Y.Y. Li, Z.S. Li, P.K. Shen, *Adv. Mater.* **25**, 2474 (2013)
19. Y. Mun, C. Jo, T. Hyeon, J. Lee, K.S. Ha, K.W. Jun, S.H. Lee, S.W. Hong, H.I. Lee, S. Yoon, J. Lee, *Carbon* **64**, 391 (2013)
20. D. Hulicova, M. Kodama, H. Hatori, *Chem. Mater.* **18**, 2318 (2006)
21. E. Frackowiak, G. Lota, J. Machnikowski, C. Vix-Guterl, F. Béguin, *Electrochim. Acta* **51**, 2209 (2006)
22. D. Hulicova-Jurcakova, M. Seredych, G.Q. Lu, T.J. Bandoz, *Adv. Funct. Mater.* **19**, 438 (2009)
23. J. Wei, D.D. Zhou, Z.K. Sun, Y.H. Deng, Y.Y. Xia, D.Y. Zhao, *Adv. Funct. Mater.* **23**, 2322 (2013)
24. Z. Liu, J.H. Mi, Y. Yang, X.L. Tan, C. Lv, *Electrochim. Acta* **115**, 206 (2014)
25. L. Qie, W.M. Chen, H.H. Xu, X.Q. Xiong, Y. Jiang, F. Zou, X.L. Hu, Y. Xin, Z.L. Zhang, Y.H. Huang, *Energy Environ. Sci.* **6**, 2497 (2013)
26. H. Zhong, F. Xu, Z.H. Li, R.W. Fu, D.C. Wu, *Nanoscale* **5**, 4678 (2013)
27. Y.C. Wang, S.Y. Tao, Y.L. An, *Microporous Mesoporous Mater.* **163**, 249 (2012)
28. G.P. Hao, J. Mi, D. Li, W.H. Qu, T.J. Wu, W.C. Li, A.H. Lu, *New Carbon Mater.* **26**, 197 (2011)
29. W. Xiong, M.X. Liu, L.H. Gan, Y.K. Lv, Y. Li, L. Yang, Z.J. Xu, Z.X. Hao, H.L. Liu, L.W. Chen, *J. Power Sources* **196**, 10461 (2011)
30. Z.B. Wen, Q.T. Qu, Q. Gao, X.W. Zheng, Z.H. Hu, Y.P. Wu, Y.F. Liu, X.J. Wang, *Electrochem. Commun.* **11**, 715 (2009)
31. H.F. Li, R.D. Wang, R. Cao, *Microporous Mesoporous Mater.* **111**, 32 (2008)
32. D.C. Wu, X. Chen, S.H. Lu, Y.R. Liang, F. Xu, R.W. Fu, *Microporous Mesoporous Mater.* **131**, 261 (2010)